CHEMIJA
2025. Vol. 36. No. 3. P. 139–149

ISSN 0235-7216 eISSN 2424-4538
DOI: https://doi.org/10.6001/chemija.2025.36.3.4

Recent advances in biomolecular analysis by ultraviolet surface-enhanced resonance Raman spectroscopy: A review

Martynas Talaikis[1, 2],

Lina Mikoliūnaitė[1],

Valdas Šablinskas[1],

Sonata Adomavičiūtė-Grabusovė[1],

Gytautė Sirgėdaitė[1],

Evaldas Stankevičius[1],

Gediminas Niaura[1, 2*]

[1] *Department of Organic Chemistry, Center for Physical Sciences and Technology (FTMC), 3 Saulėtekio Avenue, 10257 Vilnius, Lithuania*

[2] *Department of Bioelectrochemistry and Biospectroscopy, Institute of Biochemistry, Life Sciences Center, Vilnius University, 3 Saulėtekio Avenue, 10257 Vilnius, Lithuania*

Ultraviolet surface-enhanced resonance Raman spectroscopy (UV-SERRS) offers the ultrasensitive, reliable and selective analysis and sensing of biomolecules due to the combination of surface-enhancement and resonance enhancement of the Raman signal of studied molecules. In this Review, we provide the background of the technique and discuss the challenges related to ultraviolet plasmonics as well as the ability to employ the non-plasmonic substrates. We also highlight the recent applications of UV-SERRS in analysis of biomolecules. Finally, the advantages and future directions of the method are provided.

Keywords: UV-SERS, resonance, Raman, plasmonic, adenine

INTRODUCTION

Surface-enhanced Raman spectra of pyridine on the roughened silver electrode were first observed by Fleischmann, Hendra and McQuillan in 1974 [1]. They used Raman spectroscopy aiming to understand the electrochemical interface at the molecular level. Soon after that, the anomalous enhancement of Raman scattering (new phenomena) was recognised by Jeanmaire and Van Duyne [2], and Albrecht and Creighton [3]. Based on numerous efforts of physical chemists and chemical physicists, it was understood that the discovery is based on the enhancement of Raman scattering of molecules close to or in direct contact with a nanostructured plasmonic metal surface [4]. Currently, the scientific community in general agrees that two main mechanisms, electromagnetic and chemical enhancements, contribute to the SERS process. The electromagnetic (EM) enhancement results from the amplification of electric field near the nanoparticle surface

* Corresponding author. Email: gediminas.niaura@ftmc.lt

due to the excitation of localised surface plasmon resonance (LSPR) by the incident laser light [5]. Excitation of LSPR takes place when the light frequency coincides with the oscillation frequency of the electrons (plasmon resonance frequency) in the nanostructure. Plasmon resonance frequency depends on the shape, dimensions and material of the nanoparticle as well as on the dielectric environment [6, 7]. The important parameter used to describe the discovered effect is the SERS enhancement factor (EF), denoted as the magnitude of increase in the Raman cross section for a molecule adsorbed or located near the nanostructured SERS-active surface [5, 8]. The EF depends very strongly on the amplification of the local electromagnetic field (E); it scales approximately by the electric field in the fourth power – E^4 [5]. In addition, for the EM mechanism, the arrangement of plasmonic nanoparticles is important. Because of a strong electromagnetic coupling, the EF increases considerably as the distance between the plasmonic nanoparticles decreases. For example, EF increases from 10^5 to 10^9 as the distance between the gold nanospheres decreases from 10 to 2 nm [9, 10].

The chemical SERS enhancement mechanism results in an increase of polarisability of the adsorption complex [11, 12]. Three contributions can be associated with this phenomenon: (i) static chemical interactions, (ii) charge-transfer resonance (CT), and (iii) molecular resonance Raman scattering (RRS) 11]. Static chemical interaction with the substrate can increase the polarisability of the adsorbed molecule due to the structural changes and as a consequence – intensity of Raman scattering. However, in this case enhancement is relatively small, just about 10–100 times [11, 13]. The CT mechanism results from the photoinduced charge-transfer (tunnelling of electrons) from molecule-to-metal or metal-to-molecule during the SERS measurements [14, 15]. The CT phenomenon is a resonance process and strongly depends on the laser light energy, molecule energy levels, and the Fermi level of electrons in the substrate. This mechanism is valid for molecules adsorbed on metal or semiconductor surfaces [15–17]. The Raman scattering enhancement results from the resonance between the electronic transition metal(semiconductor)-molecule and the energy of the excited laser radiation. The SERS enhancement factor through the CT mechanism can reach 2–4 orders of magnitude [11]. Finally, the RRS contribution to SERS arises because of resonance between the electronic transition in the molecule at the interface and the photon of laser excitation; in this case, the combined process is named as surface-enhanced resonance Raman scattering (SERRS). The contribution from the RRS effect can be very high, reaching 4–6 orders of magnitude [11]. Indeed, many surface spectroscopic studies with adsorbed dye molecules and biomolecules in the visible spectra region, including single-molecule studies, were characterised with an extremely high sensitivity because of the operation of SERRS [8, 18, 19–21].

While the chemical mechanism at certain conditions can provide a relatively high EF, it depends strongly on the structure of the molecule and is not a universal one. On the other hand, the EM mechanism is more general and depends mostly on the structure and material of the plasmonic substrate. The overall SERS enhancement mechanism originates from the combination of EM and chemical mechanisms. Scientific community agrees that the EM mechanism provides the majority of SERS enhancement [4, 12, 23, 24].

SERS is able to provide detailed information on the structure, interactions and bonding of adsorbed molecules with a high sensitivity and selectivity [4, 5, 19–21, 25, 26]. Being one of the vibrational spectroscopy, the method provides the possibility for ultrasensitive detection and the analysis of molecules based on the fingerprint spectral pattern without the application of fluorescent probes. SERS and SERRS are widely employed in fundamental studies of the electric double layer [27–31], catalysis [32, 33], adsorption [34–37], the structure and function of self-assembled monolayers [38, 39], as well as for sensing applications in the analysis of biomolecules [40–42], pesticides [43, 44], explosives [45, 46], biomedical compounds [47–51], environmental pollutants [52, 53], and other compounds. However, a poor reproducibility, repeatability, and the interference of impurities prevent SERS applications in the analysis of 'real world' compounds and especially in biomedical laboratories and clinical studies [54, 55]. One of the possibilities toward solving this problem is the development of ultraviolet surface-enhanced resonance Raman spectroscopy

(UV-SERRS) [56, 57]. Many important organic molecules, including biomolecules, have electronic transitions in the UV spectral region. Excitation in the UV spectral region provides the possibility for the coupling of surface enhancement with the resonance Raman enhancement. Thus, UV-SERRS holds promise for the ultrasensitive detection of target biomolecules, with a low interference from various adsorbed impurities. In this review, we provide an overview of the fundamental aspects of UV-SERRS, including the mechanisms of resonance and chemical enhancement, and summarise recent progress in the development of UV-active substrates. Particular attention is given to applications in biomolecular detection and to the challenges that still limit the broader use of the method.

BACKGROUND OF UV-SERRS

UV-SERRS, which combines surface enhancement and molecular resonance enhancement mechanisms, provides the possibility for the ultrasensitive detection of certain biomolecules and organic molecules without interference from impurities. This method requires the excitation of Raman scattering in the wavelength range typically from 190 to 400 nm (UV range). The spectral region below 300 nm is named the deep ultraviolet (DUV range) [58, 59]. In the case of DUV excitation of Raman spectra at wavelengths lower than 260 nm, the fluorescence background considerably decreases [60]. This is an additional advantage of UV-SERRS spectroscopy. It should be noted that the Raman cross section of molecules in general increases in the UV spectral region because of ν^4 scattering law. Many biomolecules, including aromatic amino acids, nucleotide bases, drugs, neurotransmitters, and other organic compounds, absorb light in the UV spectral region [61]. Excitation of Raman spectra within the electronic transition results in the increase of Raman scattering by 4–6 orders of magnitude due to the RRS effect. Even if the laser radiation does not exactly coincide with the electronic transition but is close to it, the preresonance amplification of the Raman signal occurs, which can reach several orders of magnitude. For example, in the case of the adenine molecule in an aqueous solution, the main electronic transition takes place at 260 nm; however, the preresonance enhancement at 325 nm excitation wavelength results in the selective enhancement of Raman bands for 2 to 16 times [62]. The important challenge in SERS spectroscopy in the UV spectral region is the lack of efficient plasmonic material in this region. The traditional plasmonic materials such as silver, gold and copper are not efficient for SERS enhancement in the UV spectral region because of large damping due to the interband transitions [63]. Therefore, other plasmonic materials must be considered. The first UV-SERS spectra were recorded for adsorbed pyridine and SCN^- anion on roughened rhodium (Rh) and ruthenium (Ru) metal surfaces [64]. Further development in ultraviolet plasmonics revealed the suitability of many alternative materials including Al, Ga, In, Sn, Tl, Pb, Bi, Pd, and other metals [10, 63]. An alternative approach in UV-SERRS is the application of semiconducting materials, which provide an efficient chemical enhancement of Raman scattering [57].

ULTRAVIOLET PLASMONICS

LSPR properties of the metal depend on its dielectric function, which is frequency-dependent and composed from real ($\varepsilon_r(\omega)$) and imaginary ($\varepsilon_{im}(\omega)$) parts. Two important parameters characterise LSPR, i.e. plasmon resonance frequency and quality factor [65]. Metal exhibiting high-quality LSPR and a consequently large electromagnetic enhancement must possess large negative $\varepsilon_r(\omega)$ and small $\varepsilon_{im}(\omega)$ (low damping) values. Thus, the LSPR quality factor can be defined by the ratio [66]:

$$Q_1 = -\frac{\varepsilon_r(\omega)}{\varepsilon_{im}(\omega)}. \quad (1)$$

More accurate expression shows that in the small nanoparticles approximation, the quality factor (Q_2) depends only on the dielectric function at resonance frequency [65, 66]:

$$Q_2 = \left| \frac{\omega \frac{d\varepsilon_r(\omega)}{d\omega}}{2\varepsilon_{im}(\omega)} \right|. \quad (2)$$

Higher Q_2 factor results in a stronger enhancement of the local electromagnetic field near the nanoparticle. Figure 1 compares the wavelength

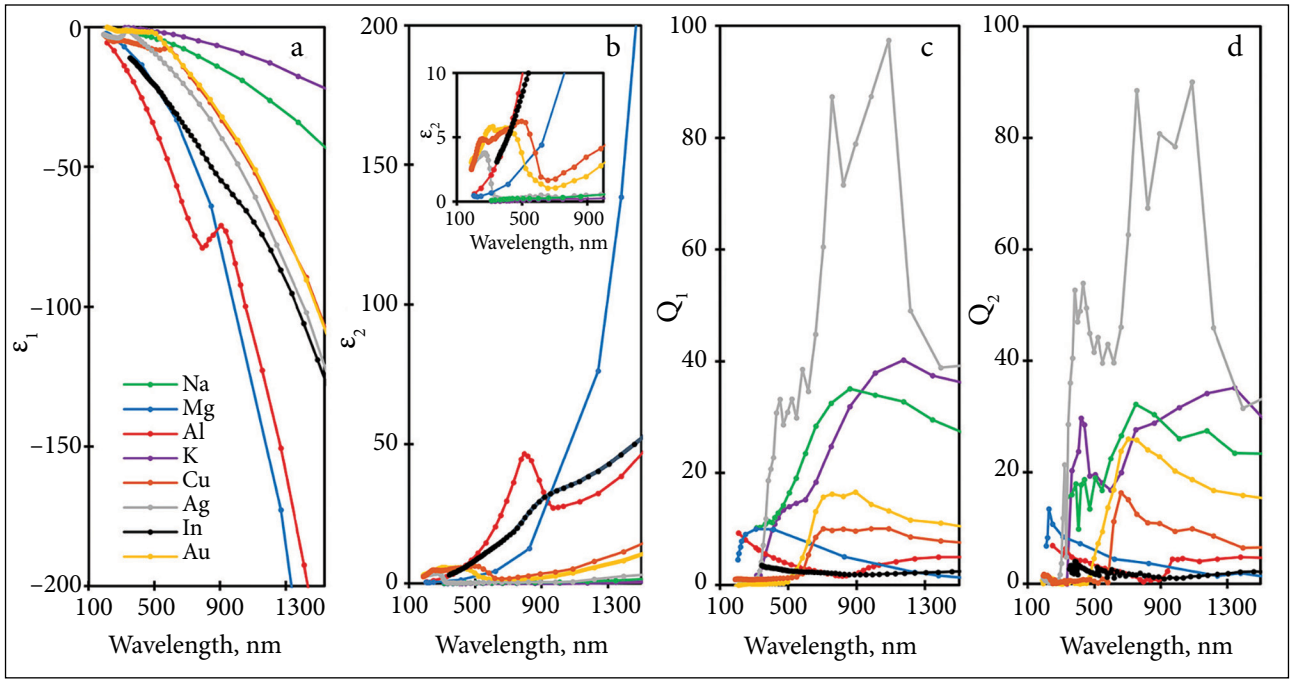

Fig. 1. Wavelength dependence of (a) real and (b) imaginary parts of dielectric function and quality factors (c) Q_1 and (d) Q_2 of Na, Mg, Al, K, Cu, Ag, In and Au metals. Reprinted from Ref. [66]

dependence of real and imaginary parts as well as quality factors of various metals. High negative ε_r values and very small ε_{im} values in the visible spectral region result in the superior plasmonic performance of Ag metal. Silver possesses the highest quality factors Q_1 and Q_2 in a broad visible spectral region in agreement with experimental SERS data. The other widely employed materials in SERS are Au and Cu. These coinage metals also show rather high Q_2 values, although at wavelengths higher than 500 nm. However, ε_{im} rapidly increases for all three coinage metals in the UV spectral region making them unusable for EM enhancement in this spectral region. The perspective plasmonic structures for this spectral region are Al and Mg; indium also shows a tendency to decrease the ε_{im} value in the UV spectral region.

The quality factors discussed above predict the wavelength range of LSPR for certain materials at a small nanoparticles approximation (electrostatic limit) [66]. This approximation is valid for nanoparticles considerably smaller compared with the wavelength of the light (the size of nanoparticles is below ~50 nm). Under this condition, the plasmon resonance frequency is related to the nature of the material, but does not depend on the size or shape of nanoparticles. However, for nanoparticles sized above ~50 nm, the properties of LSPR can be tuned by changing the size and shape of nanoparticle prepared from the same material [66, 68–70]. Remarkable progress was made in nanoscience and nanotechnology for the synthesis of the nanoparticles with various sizes and shapes [67]. Figure 2 shows how the size and shape of nanoparticles can control the plasmonic properties of different metals in a wide wavelength region [68]. Based on the analysis of 500 gold nanoparticles with a different size and shape, it was discovered that the so-called plasmon length (the length of the nanoparticle at which the plasma oscillations take place) but not the shape of the nanoparticle controls the dipolar plasmon frequency and width of the spectral bands [69]. Suitability of In, Mg and Al nanoparticles in UV plasmonics is clearly visible. In addition, silver nanoparticles of various shapes demonstrate the possibility for use in the UV spectral range down to ~340 nm. While a high chemical reactivity of Al complicates the synthesis of nanoparticles and the formation of UV-SERS substrates, numerous studies revealed the potential of this material for UV plasmonic applications [63, 71–86]. Presence of an oxide layer considerably deteriorate the plasmonic properties of aluminum (Fig. 3) [85]. Magnesium is another very chemically active, but promising material for UV-SERS [66]. Synthesis protocols of magnesium nanoparticles with controlled

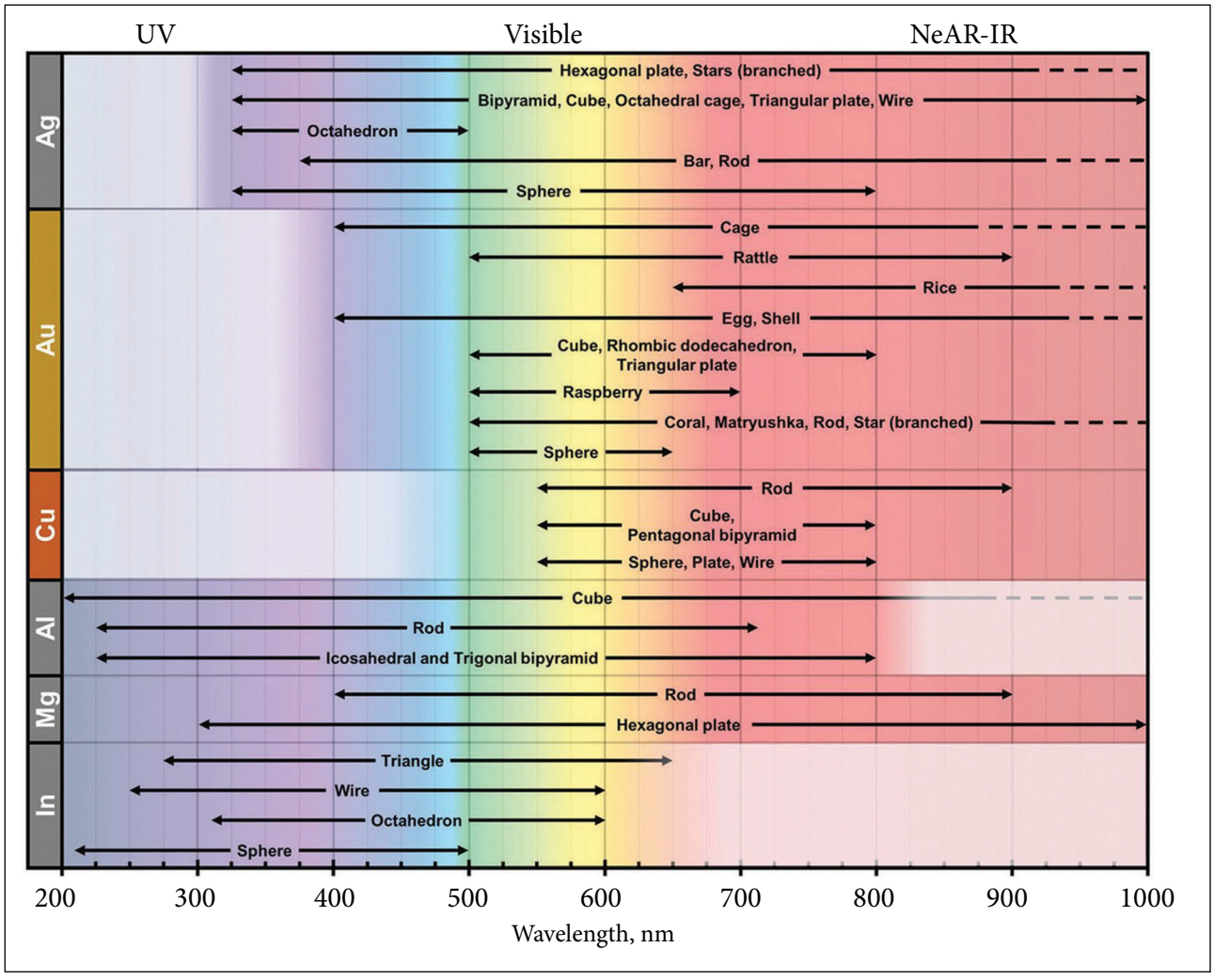

Fig. 2. Size and shape controlled plasmonic spectral range of Ag, Au, Cu, Al, Mg and In nanoparticles over the UV-Vis-NIR spectrum. Intrinsically low plasmonic performance ranges due to interband transitions are indicated by white colours. The dashed lines indicate a potential extension of the plasmon resonance in the NIR range. Reprinted from Ref. [68]

dimensions and stability were published [87–89]. Recent development of a nanoporous Al-Mg alloy film by selective dissolution of Mg from Mg-rich alloy provides the possibility for the construction of plasmonic substrate with lower oxidation level and better UV-SERS performance compared with Al structures [90]. Analysis of the dielectric function of indium in the wavelength region from 100 to 400 nm revealed the possibility for high-quality plasmon resonances in the UV spectral region for this metal because of ε_r lower than –2 and ε_{im} even smaller than that of aluminum, thus, predicting sufficiently high Q_1 [63, 91]. In particular, excellent plasmonic properties for In were predicted for the deep-UV spectral region in comparison with other metals [64]. Important advantage of In as a plasmonic material is its stability in water and compatibility with biophysical and biochemical studies [68]. Recently, Zhang et al. numerically predicted that the construction of a heterogenous dimer of Au and In nanospheres results in the improvement of plasmonic properties compared with monomer counterparts [92]. Other important metals for UV plasmonics include rhodium [63, 64, 93–97], ruthenium [64, 97], palladium [94, 98, 99], platinum [96, 99], cobalt [62, 97], gallium [63, 100], thallium [63], tin [63] and bismuth [63].

NON-PLASMONIC UV-SERRS SUBSTRATES

Various non-plasmonic substrates, including organic semiconductors, metal-organic frameworks (MOFs), copper telluride nanoparticles and 2D materials (transition metal dichalcogenides, graphene,

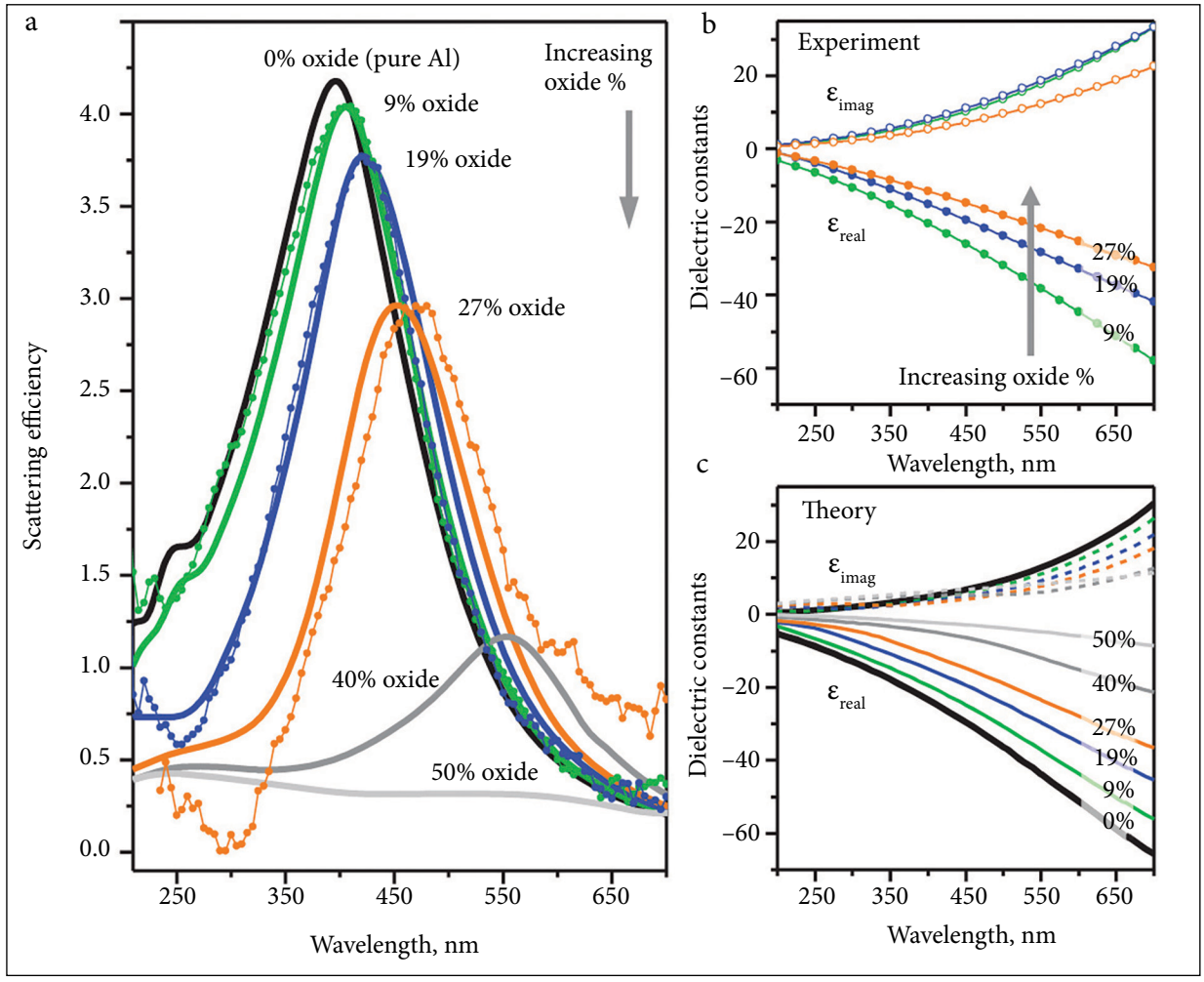

Fig. 3. Aluminum dielectric response. (a) Metal oxide-dependent scattering spectra of 100 nm nanodisks. Dotted lines are the experimental dark-field spectra, and solid lines show the calculated spectra assuming a 3 nm pure surface oxide on SiO_2. (b) Experimentally observed dielectric functions (ellipsometry). (c) Bruggemen dielectric functions. Reprinted from Ref. [85]

and titanium carbide or nitride (MXenes)) have been recently employed in SERS studies [11, 57, 67, 101, 102]. The chemical enhancement is the main Raman scattering enhancement mechanism for these materials. Possibility for the formation of semiconductor materials with tunable band gaps provides the possibility for the development of substrates with an enhanced charge transfer contribution in UV-SERRS applications [57, 103, 104]. The main advantages of these materials are (i) a high uniformity, (ii) an excellent reproducibility and (iii) an ultra-flat surface structure [103].

BIOMOLECULAR APPLICATIONS OF UV-SERRS

While the majority of UV-SERS studies were devoted to the development of effective UV plasmonic substrates, several prominent applications of the technique for the analysis of biomolecules have been published [57, 62, 94, 105–110]. Dubey and co-workers have demonstrated the possibility for reliable detection of single-base mutation in oligonucleotides by DUV-SERRS technique [105]. They employed the epitaxial Al nanohole array as a plasmonic substrate and a 266-nm deep-UV laser for the excitation of Raman scattering. The substrate was constructed to match the LSPR frequency with the excitation wavelength based on finite difference time domain analysis (100 nm diameter nanoholes with 200 nm periodicity). DUV reflectance spectra of the plasmonic substrate showed a clear reflectance minimum at 266 nm. High-quality DUV-SERRS spectra of five nucleotides (A, T, C, G and U) were observed with EF up to 10^6. Such high EF allowed for the detection of DUV-SERRS spectra

of oligonucleotides (12-mer single-stranded DNA, (ss-DNA)). Characteristic bands of different bases were clearly detected at 1339 cm^{-1} (A), 1664 cm^{-1} (T), 672 cm^{-1} (C) and 1487 cm^{-1} (G) (Fig. 4a). In addition, the single base mutation of oligonucleotides (replacement of one C base to A) was clearly visible in the spectrum of mutated 12-mer ss-DNA by a sharp 1339 cm^{-1} spectral signature (Fig. 4b). Importantly, the introduction of more mutations of A bases revealed the linear dependence of the intensity of 1339 cm^{-1} band with the number of mutations (Fig. 4c, d). The presented data demonstrate the power of the DUV-SERRS technique for the quantitative analysis of DNA mutations.

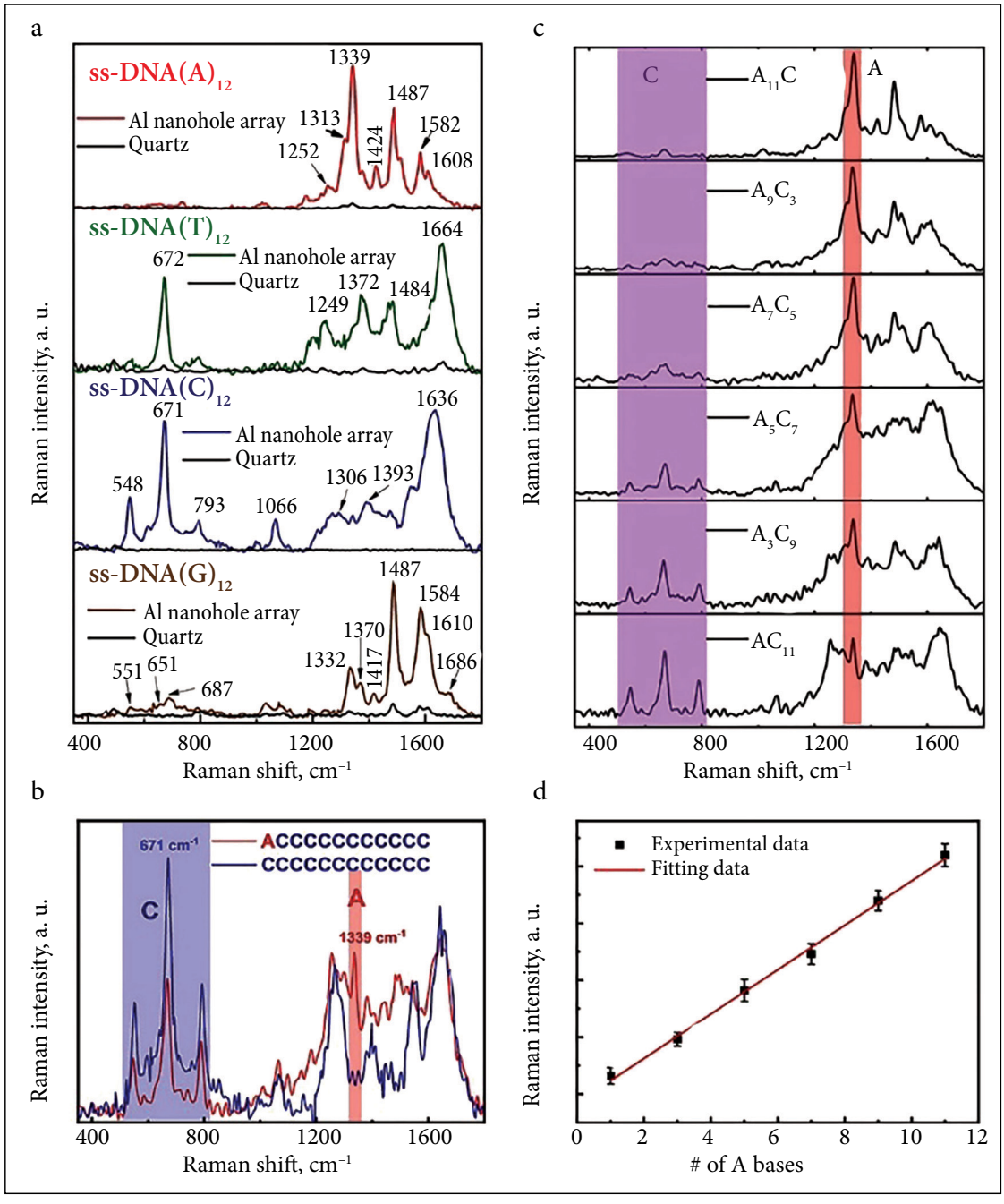

Fig. 4. (a) DUV-SERRS spectra of 12-mer single strand-DNA oligonucleotides on the Al nanohole array and quartz (black curve). (b) Comparison of DUV-SERRS spectra of initial and single base mutated oligonucleotides (CCCCCCCCCCCC and ACCCCCCCCCCC). (c) DUV-SERRS spectra of differently mutated 12-mer single-strand DNA oligonucleotides. (d) Dependence of the DUV-SERRS intensity of A-base band at 1339 cm^{-1} on the number of A bases in the 12-mer single-strand DNA oligonucleotide. Reprinted from Ref. [105]

The DUV-SERRS potency for the analysis of melamine was demonstrated by Kämmer and colleagues [107]. Various metal nanoparticles, including Pt, Pd, Au and Ag, as well as Au-Ag core-shell structures were investigated. The importance of various potassium salts for the activation of colloids was analysed. The relevance of adjusting the nanoparticle size for the detection of melamine by using DUV-SERRS was confirmed.

The power of UV-SERRS spectroelectrochemistry for the analysis of adsorbed adenine on a cobalt electrode was shown recently by Remeikiene and co-workers [62]. The electrodeposition approach was used for the development of cobalt electrode nanostructures suitable for UV plasmonics. Potential-dependent *in-situ* UV-SERRS spectra of adsorbed adenine were recorded in a wide potential region by using a 325 nm excitation wavelength. Based on the isotopic substitution effect (H_2O/D_2O), changes in solution pH, concentration and potential, the structure of the adsorbed molecule were elucidated. The predominant role of the electromagnetic enhancement mechanism in the case of UV-SERRS from the cobalt electrode was suggested. This work evidenced the perspectives of the cobalt electrode for biomolecular UV-SERRS analysis.

Copper emerged as an effective material for the UV-SERRS analysis of biomolecules [109]. The multiwavelength (229–325 nm) UV-SERRS study of various biomolecules (adenine, guanine and riboflavin) was performed on a Cu nanoparticle-based surface prepared by a wet-chemical method. The main enhancement mechanism was suggested to be chemical enhancement.

The viability of aluminum film-over-nanosphere as a plasmonic substrate for the DUV-SERRS analysis of biomolecules was demonstrated by Van Duyne group [59]. The EF was found to be high, in the order 10^{4-5}. In combination with the resonance enhancement of adsorbed biomolecules, the Raman scattering enhancement can reach values higher than 10^6. Such UV plasmonic substrates can be used for wide biomolecular UV-SERRS applications.

SUMMARY AND FUTURE DIRECTIONS

UV-SERRS technique suggests a reliable, selective and ultra-sensitive detection and analysis of biomolecules. The method can be extended for the sensing of biological markers of various diseases in biomedical and clinical studies. The main advantages of UV-SERRS include (i) the enhancement of Raman scattering efficiency according to ν^4 law, (ii) the RRS or preresonance Raman scattering for molecules with electronic transitions in the UV spectral region, (iii) the selective enhancement of chromophore bands, and (iv) the reduction in fluorescence background for excitation below 260 nm. Unlike many other analytical techniques, UV-SERRS is a label-free method, provides molecular fingerprint specificity with ultra-high sensitivity and does not require sequential procedures for the detection of certain biomarkers. The method can be applied for the in-situ and operando study of bioprocesses in a natural environment [110]. However, the poor reproducibility, signal repeatability and long-term stability of the substrates prevent the transition of the UV-SERRS method from scientific laboratories to the biomedical sites and clinics. The further development of this technique is related to the construction of reliable and easy to prepare UV plasmonic substrates (including semiconductor and 2D materials) and progress in UV-Raman instrumentation (lasers, CCD detectors and optics). The machine learning techniques could be used more widely to increase the recognition of biomolecules in mixtures and reduce the background. The possible degradation of the sample under investigation due to the UV-laser used for excitation is one of the most important concerns in the UV-SERRS field [110, 111]. The reduction of laser power and illumination time can be helpful in this respect. In addition, moving the sample or laser beam at the surface, as well as the selection of appropriate sample environment, could be explored to reduce the sample damaging [112]. We believe that further multidisciplinary efforts of scientists from fields of physical chemistry, synthetic chemistry, and nanomaterials engineering will open widely the benefits of UV-SERRS for biomedical analysis.

ACKNOWLEDGEMENTS

This work received funding from the Research Council of Lithuania (LMTLT). The project agreement number is S-MIP-23-30 'Magneto-plasmonic nanoparticles for UV-SERRS detection of low-molecular weight biomarkers (MAG-UV-SERRS)'.

DEDICATION

This article is dedicated to prof. Valdemaras Razumas on occasion of his 70 birthday in recognition of his outstanding contribution to bioelectrochemistry and biospectroscopy fields.

Received 1 September 2025
Accepted 5 September 2025

References

1. M. Fleischmann, F. J. Hendra, A. J. McQuillan, *Chem. Phys. Lett*., **26**, 163 (1974).
2. D. L. Jeanmaire, R. P. Van Duyne, *J. Electroanal. Chem*., **84**, 1 (1977).
3. M. G. Albrecht, J. A. Creighton, *J. Am. Chem. Soc*., **99**, 5215 (1977).
4. J. Langer, D. Jiminez De Aberasturi, J. Aizpurina, et al., *ACS Nano*, **14**, 28 (2020).
5. P. L. Stiles, J. A. Dieringer, N. C. Shah, R. P. Van Duyne, *Annu. Rev. Anal. Chem*., **1**, 601 (2008).
6. K. L. Kelly, E. Coronado, L. L. Zhao, G. C. Schatz, *J. Phys. Chem. B*, **107**, 668 (2003).
7. M. Li, S. K. Cushing, N. Wu, *Analyst*, **140**, 386 (2015).
8. E. C. LeRu, E. Blackie, M. Meyer, P. G. Etchegoin, *J. Phys. Chem. C*, **111**, 13794 (2007).
9. J. M. McMahon, S. Li, L. K. Ausman, G. C. Schatz, *J. Phys. Chem. C*, **116**, 1627 (2012).
10. S.-Y. Ding, J. Yi, J.-F. Li, et al., *Nat. Rev. Mater*., **1**, 16021 (2016).
11. I. Chaudhry, G. Hu, H. Ye, L. Jensen, *ACS Nano*, **18**, 20835 (2024).
12. C. Chenal, R. L. Birke, J. R. Lombardi, *ChemPhysChem*, **9**, 1617 (2008).
13. R. Chen, L. Jensen, *J. Chem. Phys*., **152**, 024126 (2020).
14. J. I. Gersten, L. R. Birke, J. R. Lombardi, *Phys. Rev. Lett*., **43**, 147 (1979).
15. J. R. Lombardi, R. L. Birke, *Acc. Chem. Res*., **42**, 734 (2009).
16. J. R. Lombardi, R. L. Birke, *J. Phys. Chem. C*, **118**, 11120 (2014).
17. Y. Liu, H. Ma, X. X. Han, B. Zhao, *Mater. Horiz*., **8**, 370 (2021).
18. C. J. L. Constantino, T. Lemma, P. A. Antunes, R. Aroca, *Anal. Chem*., **73**, 3674 (2001).
19. S. Nie, S. R. Emory, *Science*, **275**, 1102 (1997).
20. K. Kneipp, Y. Wang, H. Kneipp, L. T. Perelman, I. Itzkan, R. R. Dasari, *Phys. Rev. Lett*., **78**, 1667 (1997).
21. H. Xu, E. J. Bjerneld, M. Käll, L. Börjesson, *Phys. Rev. Let*., **83**, 4357 (1999).
22. J. Wang, C. Qui, X. Mu, H. Pang, X. Chen, D. Liu, *Talanta*, **21**, 120631 (2020).
23. S.-Y. Ding, E.-M. You, Z.-Q. Tian, M. Moscovits, *Chem. Soc. Rev*., **46**, 4042 (2017).
24. T. Itoh, K. I. Yoshida, H. Tamaru, V. Biju, M. Ishikawa, *J. Photoch. Photobiol. A Chem*., **219**, 167 (2011).
25. A. Zdaniauskiene, T. Charkova, I. Ignatjev, et al., *Spectrochim. Acta A*, **240**, 118560 (2020).
26. E. Zacharovas, M. Velička, G. Platkevičius, et al., *ACS Omega*, **7**, 10539 (2022).
27. V. Oklejas, C. Sjostrom, J. M. Harris, *J. Am. Chem. Soc*., **124**, 2408 (2002).
28. J. L. Yao, G. P. Pan, K. H. Xue, et al., *Pure Appl. Chem*., **72**, 221 (2000).
29. J. F. Li, Y. J. Zhang, A. V. Rudnev, et al., *J. Am. Chem. Soc*., **137**, 2400 (2015).
30. G. Niaura, A. Malinauskas, *Ber. Bunsenges. Phys. Chem*., **99**, 1563 (1995).
31. G. Niaura, R. Jakubėnas, *J. Electroanal. Chem*., **510** , 50 (2001).
32. B. Kazakevičienė, G. Valincius, G. Niaura, Z. Talaikytė, M. Kažemėkaitė, V. Razumas, *J. Phys. Chem. B*, **107**, 6661 (2003).
33. G. Valincius, G. Niaura, B. Kazakevičienė, et al., *Langmuir*, **20**, 6631 (2004).
34. G. Niaura, A. Malinauskas, *Chem. Phys. Lett*., **207**, 455 (1993).
35. G. Niaura, A. K. Gaigalas, V. L. Vilker, *J. Phys. Chem. B*, **101**, 9250 (1997).
36. G. Niaura, A. Malinauskas, *J. Chem. Soc. Faraday Trans*., **94**, 2205 (1998).
37. S. Martusevičius, G. Niaura, Z. Talaikytė, V. Razumas, *Vib. Spectrosc*., **10**, 271 (1996).
38. A. Bulovas, N. Dirvianskytė, Z. Talaikytė, et al., *J. Electroanal. Chem*., **591**, 175 (2006).
39. M. Kažemėkaitė, A. Bulovas, Z. Talaikytė, et al., *Tetrahedron Lett*., **45**, 3551 (2004).
40. K. C. Bantz, A. F. Meyer, N. J. Wittenberg, et al., *Phys. Chem. Chem. Phys*., **13**, 11551 (2011).
41. X. Yang, Y. He, X. Wang, R. Yang, *Appl. Surf. Sci*., **416**, 581 (2017).
42. X. Luo, Y. Xing, D. D. Galvan, et al., *ACS Sens*., **4**, 1534 (2019).
43. J. Hong, A. Kawashima, N. Hamada, *Appl. Surf. Sci*., **407**, 440 (2017).
44. S. Atta, T. Sharaf, T. Vo-Dinh, *ACS Appl. Nano Mater*., **7**, 11518 (2024).
45. Z. Gong, H. Du, F. Cheng, C. Wang, C. Wang, M. Fan, *ACS Appl. Mater. Interfaces*, **6**, 21931 (2014).
46. W. Liu, Z. Wang, Z. Liu, et al., *ACS Sensors*, **8**, 1733 (2023).
47. Z. Huang, A. Zhang, O. Zhang, D. Cui, *J. Mater. Chem. B*, **7**, 3755 (2019).
48. A. Szaniawska, A. Kudelski, *Front. Chem*., **9**, 664134 (2021).
49. A. Bonifacio, S. Cervo, V. Sergo, *Anal. Bioanal. Chem*., **407**, 8265 (2015).
50. Y. Zhang, X. Mi, X. Tan, R. Xiang, *Theranostics*, **9**, 491 (2019).

51. V. Moisoiu, S. D. Iancu, A. Stefancu, et al., *Colloids Surf. B*, **208**, 112064 (2021).
52. D.-W. Li, W.-L. Zhai, Y.-T. Li, Y.-T. Long, *Microchim. Acta*, **181**, 23 (2013).
53. T. T. X. Ong, E. W. Blanch, O. A. H. Jones, *Sci. Total Environ*., **720**, 137601 (2020).
54. A. I. Pérez-Jiménez, D. Lyu, Z. Lu, G. Liu, B. Ren, *Chem. Sci*., **11**, 4563 (2020).
55. S. E. J. Bell, G. Charron, E. C. J. Kneipp, et al., *Angew. Chem. Int. Ed*., **59**, 5454 (2020).
56. B. Sharma, R. R. Fronteira, A.-I. Henry, E. Ringe, R. P. Van Duyne, *Materials Today*, **15**, 16 (2012).
57. A. N. Giordano, R. Rao, *Nanomaterials*, **13**, 2177 (2023).
58. D. O. Sigle, E. Perkins, J. J. Baumberg, S. Mahajan, *J. Phys. Chem. Lett*., **4**, 1449 (2013).
59. B. Sharma, M. F. Cardinal, M. B. Ross, et al., *Nano Lett*., **16**, 7968 (2016).
60. S. A. Asher, C. R. Johnson, *Science*, **225**, 311 (1984).
61. Y. Kumamoto, A. Taguchi, S. Kawata, *Adv. Opt. Mater*., **7**, 1801099 (2019).
62. A. Remeikienė, I. Matulaitienė, A. Selskis, M. Talaikis, G. Niaura, *Spectrochim. Acta A*, **330**, 125733 (2025).
63. J. M. McMahon, G. C. Schatz, S. K. Gray, *Phys. Chem. Chem. Phys*., **15**, 5415 (2013).
64. B. Ren, X.-F. Lin, Z.-L. Yang, et al., *J. Am. Chem. Soc*., **125**, 9598 (2003).
65. F. Wang, Y. R. Shen, *Phys. Rev. Lett*., **97**, 206806 (2006).
66. E. P. Hopper, C. Boukouvala, J. Asseling, J. S. Biggins, E. Ringe, *J. Phys. Chem. C*, **126**, 10630 (2022).
67. O. Guselnikova, H. Lim, H.-J. Kim, et al., *Small*, **18**, 2107182 (2022).
68. N. Fontane, A. Picard-Lafond, J. Asselin, D. Boudreau, *Analyst*, **145**, 5965 (2020).
69. E. Ringe, M. R. Langille, K. Sohn, et al., *J. Phys. Chem. Lett*., **3**, 1479 (2012).
70. K. L. Kelly, E. Coronado, L. L. Zhao, G. C. Schatz, *J. Phys. Chem. B*, **107**, 668 (2003).
71. B.-W. Lin, Y.-H. Tai, Y.-C. Lee, et al., *Appl. Phys. Lett*., **120**, 051102 (2022).
72. P. Atanasov, A. Dikovska, R. Nikov, et al., *Materials*, **17**, 2254 (2024).
73. D. Su, S. Jiang, M. Yu, G. Zhang, H. Liu, M.-Y. Li, *Nanoscale*, **10**, 22737 (2018).
74. T. Ding, D. O. Sigle, L. O. Herrmann, D. Wolverson, J. J. Baumberg, *ACS Appl. Mater. Interfaces*, **6**, 17358 (2014).
75. X.-M. Li, M.-H. Bi, L. Cui, et al., *Adv. Funct. Mater*., **27**, 1605703 (2017).
76. R. D. Rodriguez, E. Sheremet, M. Nesterov, et al., *Sens. Actuators B Chem*., **262**, 922 (2018).
77. B. Sharma, M. F. Cardinal, M. B. Ross, et al., *Nano Lett*., **16**, 7968 (2016).
78. Z.-L. Yang, Q.-H. Li, B. Ren, Z.-Q. Tian, *Chem. Commun*., **47**, 3909 (2011).
79. J. Katyal, R. K. Soni, *Plasmonics*, **10**, 1729 (2015).
80. D. O. Sigle, E. Perkins, J. J. Baumberg, S. Mahajan, *J. Phys. Chem. Lett*., **4**, 1449 (2013).
81. D. Su, S. Jiang, M. Yu, G. Zhang, H. Liu, M.-Y. Li, *Nanoscale*, **10**, 22737 (2018).
82. S. S. Raja, C.-W. Cheng, Y. Sang, et al., *ACS Nano*, **14**, 8838 (2020).
83. S. K. Jha, Z. Ahmed, M. Agio, Y. Ekinci, J. F. Löffler, *J. Am. Chem. Soc*., **134**, 1966 (2012).
84. B.-W. Lin, Y.-H. Tai, Y.-C. Lee, et al., *Appl. Phys. Lett*., **120**, 051102 (2022).
85. M. W. Knight, N. S. King, L. Liu, H. O. Everitt, P. Nordlander, N. J. Halas, *ACS Nano*, **8**, 834 (2014).
86. Z. Li, C. Li, J. Yu, et al., *Opt. Express*, **28**, 9174 (2020).
87. J. Asselin, E. R. Hopper, E. Ringe, *Nanoscale*, **13**, 20649 (2021).
88. E. R. Hopper, T. M. R. Wayman, J. Asselin, et al., *J. Phys. Chem. C*, **126**, 563 (2022).
89. A. Ten, V. Lomonosov, C. Boukouvala, E. Ringe, *ACS Nano*, **18**, 18785 (2024).
90. P. Ponzellini, G. Giovannini, S. Cattarin, et al., *J. Phys. Chem. C*, **123**, 20287 (2019).
91. Y. Kumamoto, A. Taguchi, M. Honda, K. Watanabe, Y. Saito, S. Kawata, *ACS Photonics*, **1**, 598 (2014).
92. R. X. Zhang, L. Sun, C. L. Du, et al., *Physics Lett. A*, **391**, 127131 (2021).
93. D. M. Arboleda, V. Coviello, A. Palumbo, R. Pilot, V. Amendola, *Nanoscale Horiz*., **10**, 336 (2025).
94. L. Cui, D.-Y. Wu, A. Wang, B. Ren, Z.-Q. Tian, *J. Phys. Chem. C*, **114**, 16588 (2010).
95. G. Kumar, R. K. Soni, *J. Raman Spectrosc*., **53**, 1890 (2022).
96. A. Y. Zyubin, I. I. Kon, D. A. Poltorabatko, I. G. Samusev, *Nanomaterials*, **13**, 897 (2023).
97. X.-F. Lin, B. Ren, Z.-L. Yang, G.-K. Liu, Z. Q. Tian, *J. Raman Spectrosc*. **36**, 606 (2005).
98. L. Cui, S. Mahajan, R. M. Cole, et al., *Phys. Chem. Chem. Phys*., **11**, 1023 (2022).
99. L. Cui, A. Wang, D.-Y. Wu, B. Ren, Z.-Q. Tian, *J. Phys. Chem. C*, **112**, 17618 (2008).
100. Y. Yang, J. M. Callahan, T.-H. Kim, A. S. Brown, H. O. Everitt, *Nano Lett*., **13**, 2837 (2013).
101. P. K. Kannan, P. Shankar, C. Blackman, C.- H. Chung, *Adv. Mater*., **31**, 1803432 (2019).
102. C. Ji, J. Lu, B. Shan, et al., *J. Phys. Chem. Lett*., **13**, 8864 (2022).
103. M. Liu, Y. Shi, M. Wu, et al., *J. Raman Spectrosc*., **51**, 750 (2020).
104. K. Kamali, *Mater. Research Bull*., **150**, 111757 (2022).
105. A. Dubey, R. Mishra, C.-W. Cheng, Y.-P. Kuang, S. Gwo, T.-J. Yen, *J. Am. Chem. Soc*., **143**, 19282 (2021).
106. S. K. Jha, Z. Ahmed, M. Agio, Y. Ekinci, J. F. Löffler, *J. Am. Chem. Soc*., **134**, 1966 (2012).
107. E. Kämmer, T. Dörfer, Csáki, et al., *J. Phys. Chem. C*, **116**, 6083 (2012).
108. H. Pei, Y. Wei, Q. Dai, F. Wang, *Optics Commun*., **456**, 124631 (2020).

109. S. Yadav, M. Talaikis, Y. V. Ryabchikov, et al., *Adv. Optical Mater*., **13**, 2500078 (2025).
110. M. F. Cardinal, E. V. Ende, R. A. Hackler, et al., *Chem. Soc. Rev*., **46**, 3886 (2017).
111. Y. Zou, L. Mattarozzi, H. Jin, et al., *Nanoscale Adv*., **7**, 5212 (2025).
112. G. Niaura, A. K. Gaigalas, V. L. Vilker, *J. Raman Spectrosc*., **28**, 1009 (1997).

Martynas Talaikis, Lina Mikoliūnaitė, Valdas Šablinskas, Sonata Adomavičiūtė-Grabusovė, Gytautė Sirgėdaitė, Evaldas Stankevičius, Gediminas Niaura

BIOMOLEKULINIŲ ANALIZIŲ PAŽANGA TAIKANT ULTRAVIOLETINĘ PAVIRŠIAUS SUSTIPRINTĄ RAMANO SPEKTROSKOPIJĄ: PASTARŲJŲ METŲ APŽVALGA

S a n t r a u k a

Ultravioletinė paviršiaus sustiprinta rezonansinė Ramano spektroskopija (UV-SERRS), jungianti rezonansinį, paviršiaus plazmoninį ir cheminį stiprinimą, tampa perspektyviu metodu biomolekulių tyrimams. Šis metodas gali būti taikomas biologinių žymenų, susijusių su įvairiomis ligomis, nustatymui biomedicininiuose ir klinikiniuose tyrimuose, taip pat nukleorūgščių, baltymų, aminorūgščių ir kitų biologiškai bei mediciniškai svarbių junginių tyrimams. Pagrindiniai šio metodo privalumai yra Ramano sklaidos stiprinimas pagal ν^4 dėsnį, rezonansinė arba prerezonansinė Ramano sklaida molekulėms, kurių elektroniniai šuoliai patenka į UV sritį, selektyvus chromoforinių centrų virpesinių juostų sustiprėjimas bei sumažėjęs fluorescencijos fonas, kai žadinančios spinduliuotės bangos ilgis yra trumpesnis nei 260 nm. Tolesnė šios metodikos plėtra siejama su patikimų ir paprastai paruošiamų UV plazmoninių padėklų kūrimu, ypač naudojant aliuminį, indį, magnį, rodį, paladį, kobaltą ar jų lydinius, taip pat puslaidininkines medžiagas. Didelę reikšmę turi ir UV Ramano aparatūros (lazerių, CCD detektorių ir optikos) vystymasis. Vis dėlto esminiu iššūkiu išlieka mėginių degradacija, kai jie žadinami UV lazeriu, o ši problema tebėra svarbi kliūtis tolimesnei UV-SERRS metodikos plėtrai.